

Ferroptosis-related genes DUOX1 and HSD17B11 affect tumor microenvironment and predict overall survival of lung adenocarcinoma patients

Chunhui Wei, MM^a, Lixia Li, PhD^b, Youping Qiao, MM^a, Yujuan Chen, MM^a, Chunfeng Zhang, MM^a, Jinye Xie, MM^a, Jiayan Fang, MM^a, Zhu Liang, MM^c, Dan Huang, PhD^{a,b}, Dong Wu, PhD^{a,*}

Abstract

Background: Recent studies have found that ferroptosis-related genes (FRGs) have broad applications in tumor therapy. However, the predictive potential of these genes in lung adenocarcinoma (LUAD) remains to be fully characterized. We aimed to investigate the FRGs that might be potential targets for LUAD.

Methods: We screened the RNA sequencing samples from LUAD patients from the GEO database and analyzed the ferroptosis-related differentially expressed genes (DEGs). A functional analysis of DEGs was performed. The risk model was constructed to evaluation and validation FRGs. We explored the immune landscape of LUAD and controls. The value of FRGs in diagnosing LUAD was tested in the GSE30219, GSE37745, GSE0081 datasets, and qPCR was used to verify their diagnostic value in LUAD patients in our hospital.

Results: A total of 1327 DEGs in quantitative proteomics were obtained, of which ferroptosis-related DEGs were 259. Enrichment analysis showed significant enrichment in the absorption and metabolism of fatty acids and arachidonic acid. The upregulated genes (GCLC, RRM2, AURKA, SLC7A5, and SLC2A1) and downregulated genes (ANGPTL7, ALOX15, ALOX15B, HSD17B11, IL33, TSC22D3, and DUOX1) were selected as core genes in tissue samples from 62 patients by qPCR. DUOX1 and HSD17B11 were obtained by bioinformatics analysis, both of which showed similar expression trends at the RNA and protein levels. The Kaplan–Meier method showed that DUOX1 and HSD17B11 were closely related to the overall survival (OS) of LUAD patients.

Conclusion subsections: Ferroptosis-related genes DUOX1 and HSD17B11 are of considerable value in the diagnosis of LUAD patients. Their low expression suggests an increased recurrence rate and leads to a decrease in the patient quality of life.

Abbreviations: DEGs = differentially expressed genes, DEPs = differentially expressed proteins, DUOX1 = dioxase 1, FRGs = ferroptosis-related genes, GPX4 = glutathione peroxidase 4, LDs = lipid droplets, LUAD = lung adenocarcinoma, NSCLC = non-small cell lung cancer, OS = overall survival, PCA = principal component analysis, ROS = reactive oxygen species, RS = scores, TME = tumor microenvironment.

Keywords: DUOX1, ferroptosis, HSD17B11, lung adenocarcinoma, proteomics

1. Introduction

The latest cancer data show that the incidence and mortality of lung adenocarcinoma (LUAD) have dropped sharply in recent years, but still high.^[1] The most common type of non-small cell

lung cancer (NSCLC) is LUAD, which accounts for about 40%.^[2] In general, the treatment of LUAD consists of 5 approaches: immunotherapy, gene-targeted therapy, chemotherapy, radiotherapy, and surgical resection.^[2,3] Therapeutic surgery is the first choice for most patients with early and advanced NSCLC,

This work was supported by grants from the Affiliated Hospital of Guangdong Medical University "Clinical Medicine+" CnTech Co-operation Project (Grant Number CLP2021B001, CLP2021B017), the Discipline Construction Project of Guangdong Medical University (Grant Number 4SG21231G), Guangdong Provincial Administration of Traditional Chinese Medicine (20221211), the Project of Zhanjiang City (Grant Number 2018A01025, 2020A01016, 2020B01346 and 2021A05052), the Doctoral Start-up Project of Affiliated Hospital of Guangdong Medical University (BK201605), Guangdong Provincial Medical Scientific Research Fund (B2019206).

The authors have no conflicts of interest to disclose.

The datasets generated during and/or analyzed during the current study are not publicly available, but are available from the corresponding author on reasonable request.

All patients signed informed consent forms, and the Ethics Committee of the Affiliated Hospital of Guangdong Medical University approved the study.

^a Department of Respiratory and Critical Care Medicine, Affiliated Hospital of Guangdong Medical University, Zhanjiang, China, ^b Cancer Hospital, Affiliated Hospital of Guangdong Medical University, Zhanjiang, China, ^c Department of

Cardiothoracic Surgery, Affiliated Hospital of Guangdong Medical University, Zhanjiang, China.

* Correspondence: Dong Wu; Department of Respiratory and Critical Care Medicine, Affiliated Hospital of Guangdong Medical University, 57th South Renmin Road, Zhanjiang 524001, China (e-mail: wudong98@126.com).

Copyright © 2024 the Author(s). Published by Wolters Kluwer Health, Inc. This is an open-access article distributed under the terms of the Creative Commons Attribution-Non Commercial License 4.0 (CCBY-NC), where it is permissible to download, share, remix, transform, and build up the work provided it is properly cited. The work cannot be used commercially without permission from the journal.

How to cite this article: Wei C, Li L, Qiao Y, Chen Y, Zhang C, Xie J, Fang J, Liang Z, Huang D, Wu D. Ferroptosis-related genes DUOX1 and HSD17B11 affect tumor microenvironment and predict overall survival of lung adenocarcinoma patients. *Medicine* 2024;103:22(e38322).

Received: 14 January 2024 / Received in final form: 4 March 2024 / Accepted: 1 May 2024

<http://dx.doi.org/10.1097/MD.000000000038322>

and advances in targeted therapies and the advent of immunotherapy have benefited many patients, but their long-term clinical efficacy is affected by the molecular heterogeneity of lung cancers and acquired resistance, and the overall survival rate is still very low.^[4] To further improve the prognosis, there is an urgent need to find targeted prognostic prediction methods for LUAD patients in order to design supportive treatment and management programs for patients with different subtypes of LUAD.^[3] In recent years, ferroptosis has shown great potential in cancer therapy, with various tumor cells being sensitive to ferroptosis and rapid development of ferroptosis inducers, suggesting that ferroptosis may have considerable potential in tumor therapy and prognosis prediction.^[5,6] Programmed cell death dominated by ferroptosis, distinct from necrosis and apoptosis, is characterized by the accumulation of intracellular iron ions and lipid peroxides, and also involves a dysfunctional balance of scavenging mechanisms and an increase in reactive oxygen species (ROS).^[7] Immortalization of tumor cells requires massive energy expenditure, an environment of dramatic biochemical metabolic imbalance and accumulation of toxic substances. These features are closely associated with ferroptosis, suggesting that ferroptosis is one of the factors to which tumor cells are highly sensitive.^[8] Ferroptosis has been proved to be associated with cancer treatment resistance, and inhibition of ferroptosis-related proteins, such as glutathione peroxidase 4 (GPX4), is beneficial to development of drug resistance and tumor recurrence.^[9,10]

The use of immunotherapies to treat cancer is currently generating a large amount of attention. Yiru Wang et al and Weimin Wang et al separately found that CD8 + T cells can enhance immunotherapy by triggering ferroptosis through the downregulation of SLC3A2 and SLC7A11.^[11,12] This suggests that targeting ferroptosis could represent a new therapeutic strategy, as ferroptosis has been shown to be closely linked to a number of cancers.^[13,14] Recent studies have used bioinformatics to identify ferroptosis-related genes (FRGs) and to relate them to tumor prognosis using data from public databases, leading to the construction of prognostic prediction models.^[15] However, the role of FRGs in LUAD still unclear.

In this study, we used quantitative proteomics in combination with bioinformatics to screen for FRGs associated with LUAD prognosis, and then verified them by analyzing clinical samples from patients with LUAD.

2. Materials and methods

2.1. Collection and preservation of human tissue samples

The tissues of patients who were diagnosed as LUAD for the first time from 2021 to 2023 and underwent surgical treatment were collected and stored in liquid nitrogen, and the clinical information of all patients was obtained, including gender, age, smoking status, internal diameter, tumor, lymph node and metastasis staging, clinical staging and 5-year survival rate information. A total of 62 cases were collected, each of which contained cancerous tissues and adjacent tissues. All patients signed the informed consent form, and the research was approved by the Ethics Committee of the Affiliated Hospital of Guangdong Medical University.

2.2. Quantitative proteomic analysis of human tissue samples

We performed quantitative proteomic analysis of samples from 3 patients diagnosed with LUAD. Cancer and adjacent tissue samples from the 3 patients were lysed and digested to extract the total protein content. The digested peptides from each sample were then desalted, concentrated, recombined, and labeled with iTRAQ reagents (Applied Biosystems). The labeled

peptides were isolated using the AKTA Purifier System (GE Healthcare). The labeled peptides were put into a Q Exactive mass spectrometer (Thermo Scientific) for LC-MS/MS analysis. MASCOT engine (Matrix Science, London, UK; Version 2.2) is used to search for sample data, and the data is identified and quantitatively analyzed in protein Group Finder 1.4 software.

2.3. Bioinformatic methods to identify major FRGs associated with LUAD prognosis

2.3.1. Data download and preprocessing. The UCSC website (<http://xena.ucsc.edu/public/>) extracts level 4 gene expression data from LUAD patients. The GSE30219, GSE37745 and GSE50081 datasets (including clinical follow-up information) were obtained from the public repository GEO database, and the tool for background adjustment and data normalization was the limma software package. When pre-processing RNA sequencing samples from LUAD patients, we used TCGA and GEO data to exclude patients with unclear or missing clinical outcomes, such as survival time or survival status. After preprocessing, we obtained 500 samples from total LUAD and 293, 196, and 181 samples from the GSE30219 dataset, GSE37745 dataset, and GSE50081 dataset, respectively. In addition, 259 FRGs were obtained from FerrDb.^[16]

2.3.2. LUAD subtypes and risk groups. The gene expression matrix of 259 FRGs was determined by RNA-seq data from TCGA-LUAD. LUAD prognosis-related genes were identified at R (www.r-project.org) ($P < .05$). We used ConsensusClusterPlus (V1.56.0) to consistently cluster LUAD patients (parameters: rep = 100, pItem = 0.8, pFeature = 1, distance = Pearson). Then we classified the data according to the optimal k value. Random Forest package in R can be used to construct classification models and screen FRGs to identify those that contribute most to the classification model.^[17,18] Patients in the TCGA-LUAD cohort followed a random assignment principle to be disrupted into either the training or test cohort at a ratio of 7:3 (350:150), and cross-validation was used to retain the minimum number of FRGs to minimize the interpretable variance. We computed multivariate Cox regression analyses using the R package and then used a random forest classifier to compute risk scores (RS) for each FRG ($RS = \sum \beta_{FRGs} \times Exp_{FRGs}$), where β_{FRGs} represents the estimated contribution coefficient of FRGs in the regression analysis and Exp_{FRGs} represents the expression level of FRGs.

2.3.3. Functional analysis of different LUAD subtypes. Data describing somatic gene mutations and copy number mutations were obtained from the UCSCXena website. The distribution of somatic gene mutations in LUAD subtypes was compared using Fisher test in the maftools package. P values $< .05$ were statistically different. Each LUAD sample contained 22 immune cell phenotypes, and the level of immune infiltration of different cell subtypes and RS groups in samples with $P < .05$ was assessed using CIBERSORT (<https://cibersortx.stanford.edu/>). The ESTIMATE package was used to calculate ImmuneScore, StromalScore, and EstimateScore, the first 2 corresponding to the immune and stromal components of the tumor microenvironment (TME), with higher scores being associated with larger ratios. The EstimateScore is the sum of the 2, indicating the combined ratio.

2.3.4. Screened differentially expressed genes and regulatory signaling pathways. The edgeR package implements statistical analysis based on a negative binomial distribution, which was used to estimate gene expression changes in different LUAD subtypes, and finally displayed as a volcano plot. Samples with an adjusted $P < .05$ and $|\log_2(\text{fold change})| > 1.5$ were defined as differentially expressed genes (DEGs). GO enrichment

analysis was used to query the functional enrichment of LUAD cancer cells, whereas KEGG enrichment observes the pathway enrichment in order to facilitate the screening of pathways. The above functions require the clusterProfiler package and the GSEA package, respectively.

2.4. RT-qPCR

Cancer tissues collected from 62 LUAD pairs were sorted with adjacent tissue labeling sequences, from which total RNA was extracted using TRIzol Reagent (Invitrogen, CA). RT-qPCR was performed according to the procedure and analyzed on an ABI7500 (Applied Biosystems, Foster City, CA). GAPDH was used as a normalized control and the primers are shown in Table 1 (Sanko Biotech, Shanghai, China).

2.5. Statistics

We used the R program (version 4.0.1) and GraphPad Prism 8.0 for statistical analysis. Wilcoxon signed-rank test was used to compare the means of 2 groups, and Kruskal-Wallis test was used for more than 2 groups. Measurement data were analyzed by t-test or one-way ANOVA, and categorical variables were analyzed by Chi-square test and Fisher test. Kaplan–Meier was used for survival analysis. Data were expressed as mean ± standard deviation, and *P* < .05 was statistically significant.

3. Results

3.1. Differentially expressed proteins (DEPs) were identified by quantitative proteomics

The quantitative proteomic flow of DEPs in LUAD patients is shown in Figure 1A. We identified 1327 DEGs from 7930 proteins after LC-MS/MS analysis of labeled peptides in paired tissue samples from 3 LUAD patients (Fig. 1A and B). Up-regulated proteins accounted for 783 and down-regulated proteins accounted for 544 of the 1327 DEGs (Fig. 1C). The differential screening criteria were: up-regulation over 1.2-fold or down-regulation over 0.83-fold, *P* < .05.

3.2. FRGs were associated with overall survival (OS) in LUAD patients

We initially obtained 259 FRGs from FerrDb. In order to identify ferroptosis-related proteins from the identified DEGs that were linked to patient prognosis, we used bioinformatics to analyze whether FRGs could have an impact on OS. 28

FRGs were correlated with OS after evaluation using univariate Cox proportional regression analysis (*P* < .05). We looked at the clustering based on the expression of these 28 FRGs in the TCGA-LUAD cohort, and showed that the patients were clearly divided into 2 subtypes when *k* = 2 (cluster_1 and cluster_2; Fig. 2A). Principal component analysis (PCA) further confirmed the results of dimensionality reduction of these 2 subtypes by linear transformation (Fig. 2B). The heatmap clearly showed that the expression of FRGs was significantly different in these 2 subtypes (Fig. 2C), and the OS of LUAD patients was improved in cluster_1 compared to cluster_2 (*P* < .0001; Fig. 2D).

We next screened the core FRGs to identify those that were sufficient to classify LUAD patients into either cluster_1 or cluster_2, and found 12 FRGs that were closely correlated with classification. These 12 FRGs were: SLC2A1, SLC7A5, GCLC, RRM2, AURKA, TSC22D3, HSD17B11, ALOX15B, DUOX1, IL33, ALOX15, and ANGPTL7 (Fig. 2E and F). We then used multivariate Cox proportional risk regression in the survminer software package to derive a risk score for each core FRG. LUAD patients were categorized into high-risk and low-risk groups according to the level of risk score. This was done to obtain the survival status of patients with different RS. The survival curves of the high-risk group moved consistently lower than those of the low-risk group, suggesting that the OS rate was lower in the high-risk group (Fig. 2G). In addition, the heatmap showed that FRGs TSC22D3, HSD17B11, ALOX15B, DUOX1, IL33, ALOX15, and ANGPTL7 were down-regulated in the high-risk group, contrary to those in the low-risk group (Fig. 2H).

3.3. The potential biological functions of FRGs in LUAD patients

To explore the biological functions of the FRGs, we analyzed the genes that were differentially expressed between the 2 subtypes, and looked at the regulatory signaling pathways that may be related. We used the edgeR package to compare the gene expression levels between the 2 subtypes and eliminated 1059 DEGs, including 738 upregulated and 321 downregulated genes (Fig. 3A). GO and KEGG enrichment analysis showed that these DEGs were mainly involved in nuclear fission, chromosome segregation, and other cellular activities, such as the absorption and metabolism of fatty acids and arachidonic acid. These DEGs were also closely related to pathways such as the regulation of the cell cycle, DNA replication, DNA mismatch repair, and linolenic acid metabolism (Fig. 3B–D). Together, these data suggest that the differential expression of FRGs between cluster_1 and cluster_2 may be related to somatic gene mutations. We, therefore, analyzed the differences in somatic mutational profiles and the tumor mutational burden between LUAD subtypes and found that cluster_2 (containing patients with a poorer prognosis) had a higher mutation rate. Together, these findings further support that the differential expression of FRGs is associated with OS in LUAD patients (Fig. 3F). The top 16 genes with the highest mutation frequency in the 2 subtypes are shown in (Fig. 3G).

3.4. FRGs could affect the TME of LUAD

The relationship between ferroptosis and TME is of some importance for cancer cell survival. To examine this, we investigated the effect of the FRGs on the TME of LUAD tumors. We used CIBERSORT to assess the level of immune infiltration, looked at ImmuneScore, StromalScore, and EstimateScore scores to evaluate the proportion of the corresponding components, finally analyzed their correlation with OS. An increase in the level of both immune and stromal components of the TME typically correlated with better rates of OS, which tentatively suggests that an increase in FRGs in LUAD patients was favorable

Table 1
Sequence of primers were used in this study.

Genes	Forward (5' to 3')	Reverse (5' to 3')
GCLC	CGCAGGTTTTGGTCACA	GCTCCCGCTTCTCTTTG
TSC22D3	GGTGCCAAGAGATGCCTA	ATGCAACTCAGCCTCCA
ALOX15	CTCATCTTCTGAGGGGACA	TTCAGGGGTATCGCA
ANGPTL7	TCTCCTTCTACCGGGACTG	TCCTCCATCTTACACGCA
ALOX15B	GGACACCCTGACCCTGAA	CGCCGTAGAGAGCTGGA
DUOX1	TGGCTGACAAGGATGGC	GCGGAACATAAGGCAGA
SLC7A5	TTTGGAGGCTGAGTTCTGG	CATTGGAGGCTGAGGGTAG
AURKA	TCTCTGGTGGCATTCCCT	ATGGCCTCTCTGTATCCC
RRM2	GAAAACCTGGTGGAGCGA	GCGGGCTTCTGTAATCTG
HSD17B11	GACATCCTCCTGCTTCTCC	ATGCCAGCTCCTGTAATC
SLC2A1	CACCGCTATGGGGAGAG	CCACAGAGAAGGAGCCAA
IL-33	AGAGAAACCACAAAAGGC	ATACCAAAGGCCAAGCACTC

DUOX1 = dioxase 1.

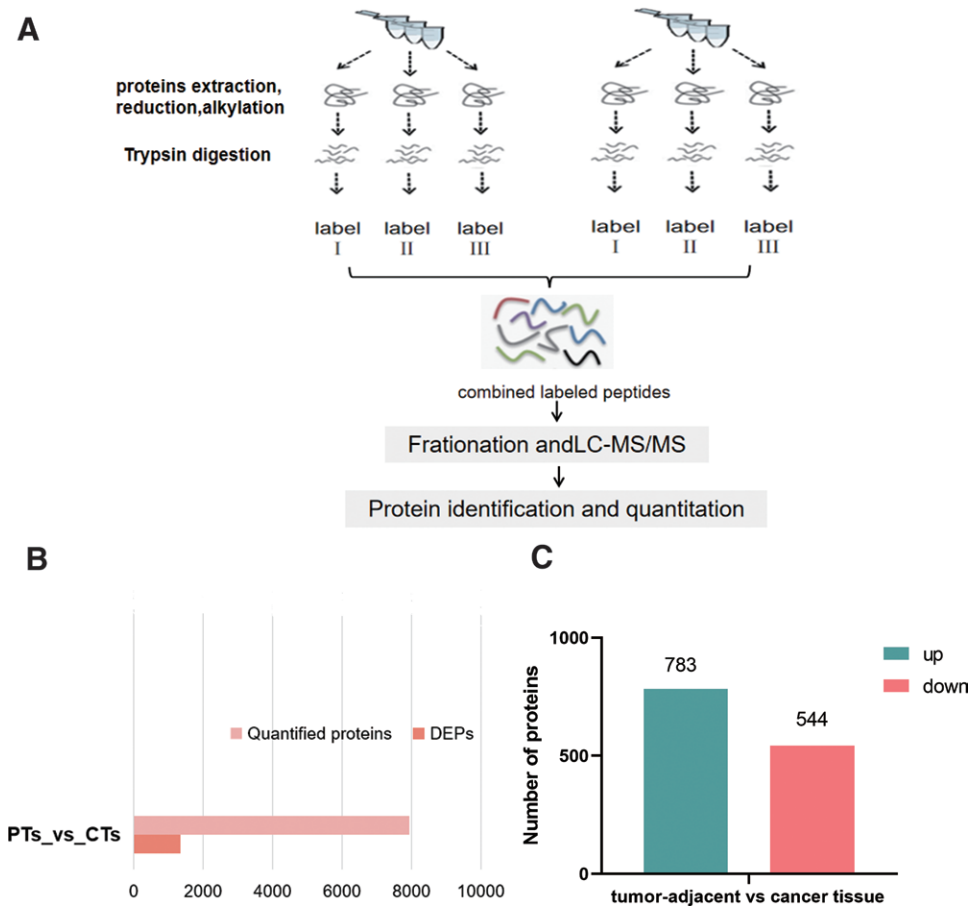


Figure 1. Quantitative proteomic verification of DEPs in LUAD patients. (A) Flow chart showing the quantitative proteomic workflow. (B) The total number of the 7930 proteins quantified is shown in light red, and the proportion that was differentially expressed is shown in orange. (C) Of these differentially expressed genes, the 783 proteins that were upregulated are shown in green, and the 544 proteins that were downregulated are shown in red. DEPs = differentially expressed proteins, LUAD = lung adenocarcinoma.

(Fig. 4A–F). For further validation and to identify associations, we proceeded to analyze the specifics of the immune infiltration of 22 immune cell subpopulations. There are 14 immune cell types found in cluster_1 and cluster_2 that may be associated with LUAD subtypes. The cell types enriched in cluster_1 were predominantly resting memory CD4 T cells, monocytes, and mast cells, whereas cluster_2 contained nonproliferating cells such as macrophage M0 (Fig. 4G). We generated heatmaps showing the correlation between the expression of the 12 core frg and different types of immune cells (Fig. 4H). These data all support the hypothesis that FRGs may affect the LUAD TME.

3.5. Gene expression level of 12 FRGs in LUAD patients

We verified the gene express patients by RT-qPCR and found that GCLC, RRM2, AURKA, SLC7A5, and SLC2A1 were upregulated in cancerous compared to paracancerous tissues (all $P < .05$; Fig. 5A–E), while ANGPTL7, ALOX15, ALOX15B, HSD17B11, IL33, TSC22D3, and DUOX1 were downregulated (all $P < .05$; Fig. 5F–L). ion levels of 12 core FRGs in tissue samples from 62 LUAD

3.6. DUOX1 and HSD17B11 are downregulated, at both RNA and protein levels, and are associated with poorer prognosis for LUAD patients

To further characterize the FRGs that show consistent differences in both RNA and protein levels in LUAD tumors

compared to healthy cells, we compared the 1327 DEGs identified by proteomics with the 12 core FRGs identified by bioinformatic analysis, and obtained 2 FRGs: DUOX1 and HSD17B11 (Fig. 6A and B). Both DUOX1 and HSD17B11 were downregulated at the RNA and protein levels, and may be associated with poorer prognosis for LUAD patients. In the case of verifying the above conjecture, 62 LUAD patients were categorized into these 2 groups showing high or low protein expression according to their median expression levels (clinical characteristics of these patients are displayed in Table 2). From the Kaplan–Meier curves we can see that the OS of LUAD patients with low levels of either DUOX1 or HSD17B11 was significantly shorter than for patients with high levels of the 2 genes (600 days vs 810 days; 630 days vs 780 days, all $P < .05$) (Fig. 6C and D).

4. Discussion

With the advancement of medical technology and the maturation of gene-targeted therapy and immunotherapy techniques, the quality of survival and survival outcomes of lung cancer patients have improved dramatically.^[19] However, long-term use will inevitably lead to drug resistance in cancer cells, which has caused great concern. The previous work on ferroptosis has indicated that ferroptosis leads to widespread tumor cell death, and thus, targeting the induction of ferroptosis may be a novel cancer treatment strategy to improve patient OS. In response to this question, we first used proteomics and public databases (including FerrDb, GEO, and TCGA) to identify 12 core FRGs that are strongly associated with OS in LUAD patients (SLC2A1,

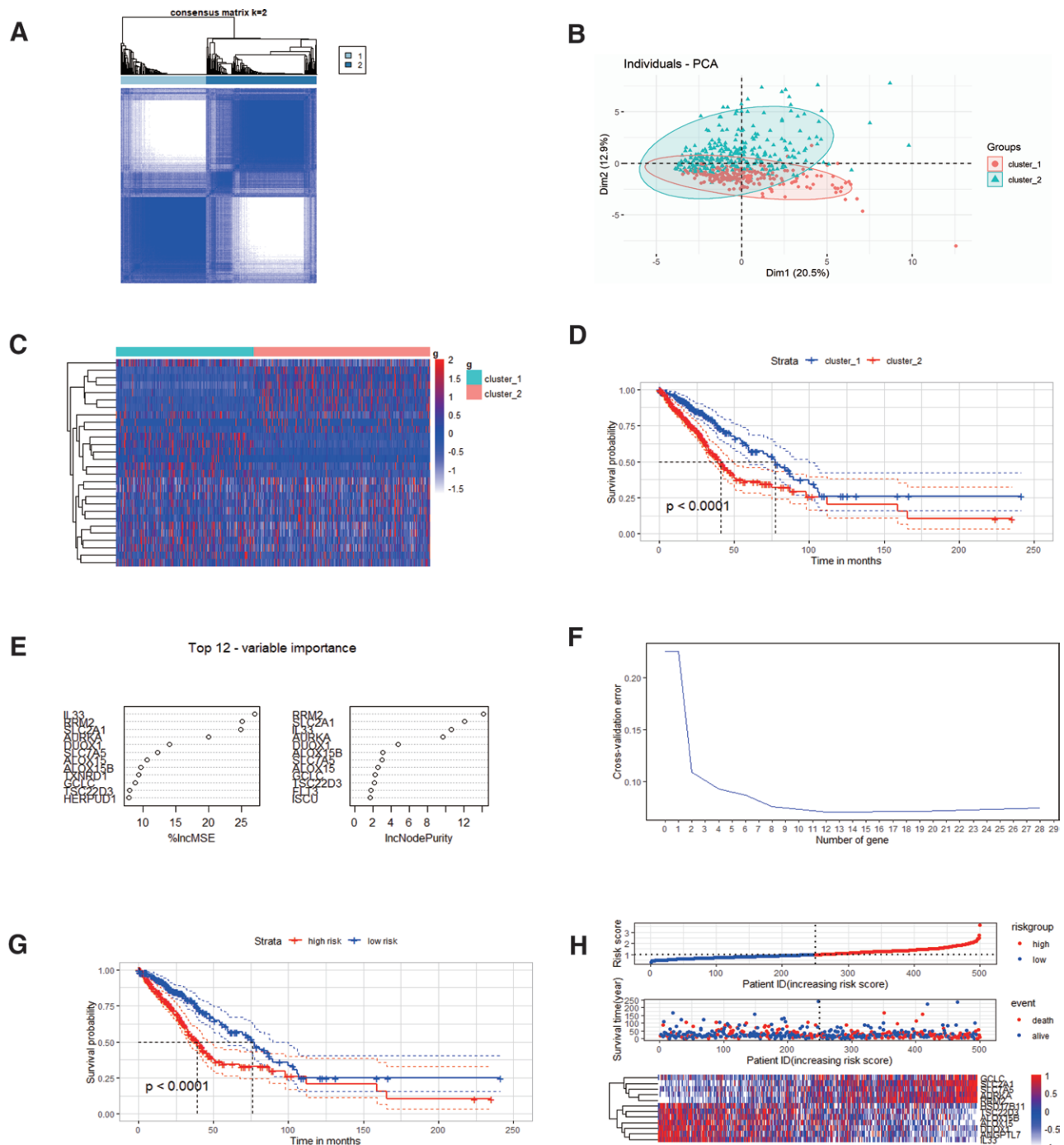


Figure 2. 12 FRGs related to the prognosis of LUAD were identified. (A) Consistent cluster analysis when $k = 2$. (B) LUAD subtypes visualized in PCA. (C) Heatmap showing the expression of the prognosis-related FRGs. (D) Kaplan–Meier curves showing OS for different subtypes. (E) Top 12 FRGs. (F) The number of genes that minimize explained variance. (G) Survival analysis of different risk groups. (H) The relationships between different risk scores and FRGs. FRGs = ferroptosis-related genes, LUAD = lung adenocarcinoma, OS = overall survival.

SLC7A5, GCLC, RRM2, AURKA, TSC22D3, HSD17B11, ALOX15B, DUOX1, IL33, ALOX15, ANGPTL7). These 12 core FRGs were further screened in lung cancer cells and the related proteins DUOX1 and HSD17B11 were obtained to be down-regulated in cancer cells. Low expression of DUOX1 or HSD17B11 was correspondingly demonstrated to be associated with low OS in clinical samples.

Cancer cells are inevitably affected by oxidative stress during growth. Cancer cells under oxidative stress inhibit the synthesis of glutathione (the most abundant cellular antioxidant in cells), and GPX4 is inactivated due to a lack of raw materials,

accelerating the accumulation of lipid peroxidation to a level that can induce ferroptosis. Lipid metabolism, which is involved in the ferroptosis process, is also integral to cancer cells.^[20] It provides cancer cells with energy for biological activities, biofilm components, lipid nutrients, and oxidative stress environment, which contributes to rapid proliferation, prolonged survival, and strong migratory invasive capacity of cancer cells.^[21] These findings support the idea that cancer development, progression and suppression are all influenced by ferroptosis.^[22] Inspired by this view, we used GO and KEGG enrichment analyses to identify genes that showed differential expression between LUAD

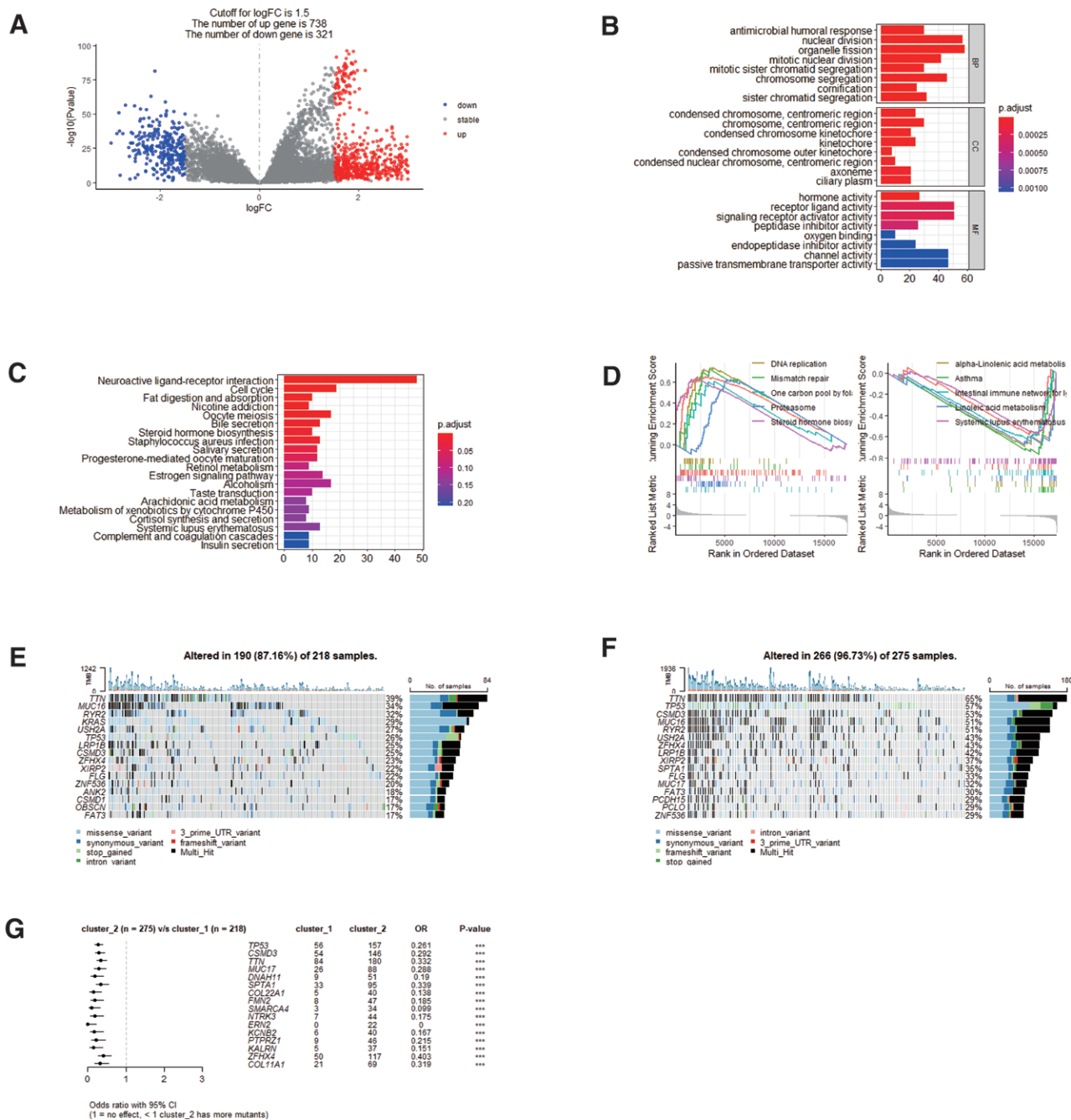


Figure 3. The potential biological functions of FRGs in LUAD patients. (A) Volcano plot showing differentially expressed genes. (B) GO functional enrichment analysis of DEGs. (C) KEGG functional enrichment analysis of DEGs. (D) GSEA pathway enrichment analysis of DEGs. (E, F) Somatic mutations in different LUAD subtypes. (G) The 16 genes with the highest mutation frequency in different subtypes. DEGs = differentially expressed genes, FRGs = ferroptosis-related genes, LUAD = lung adenocarcinoma.

patients with poor OS rates compared to patients with better rates of OS, and to show that a number of these genes are related to the absorption and metabolism of fatty acids and arachidonic acid. Moreover, the FRGs that we identified were also involved in these metabolic pathways.

Previous studies have shown that immune cell infiltration in the TME is associated with cancer progression and patient survival.^[2,3-25] Uncovering how immune cells in the TME respond and adapt to lethal lipid peroxidation may help to understand the role of ferroptosis in cancer immunity, and further to promote the development of ferroptosis-targeted therapies.^[26] The TME is enriched in many different types of immune cells, including tumor-associated macrophages, natural killer cells,

and T cells, which are essential for maintaining iron homeostasis.^[27] In this study, we found that CD4 memory resting T cells, resting mast cells, monocytes, and macrophages (M0) were strongly associated with LUAD prognosis, and were also significantly associated with the expression levels for 12 FRGs. These findings suggest that ferroptosis may be a potential target for cancer immunotherapy. Wang *et al* showed that CD8 + T cells can regulate tumor ferroptosis during tumor immunotherapy, and promoting ferroptosis can help improve the efficacy of immunotherapy.^[11]

Cancer development, progression and suppression may be influenced by ferroptosis.^[22] Cancer cells subjected to oxidative stress exert an inhibitory effect on glutathione (the most

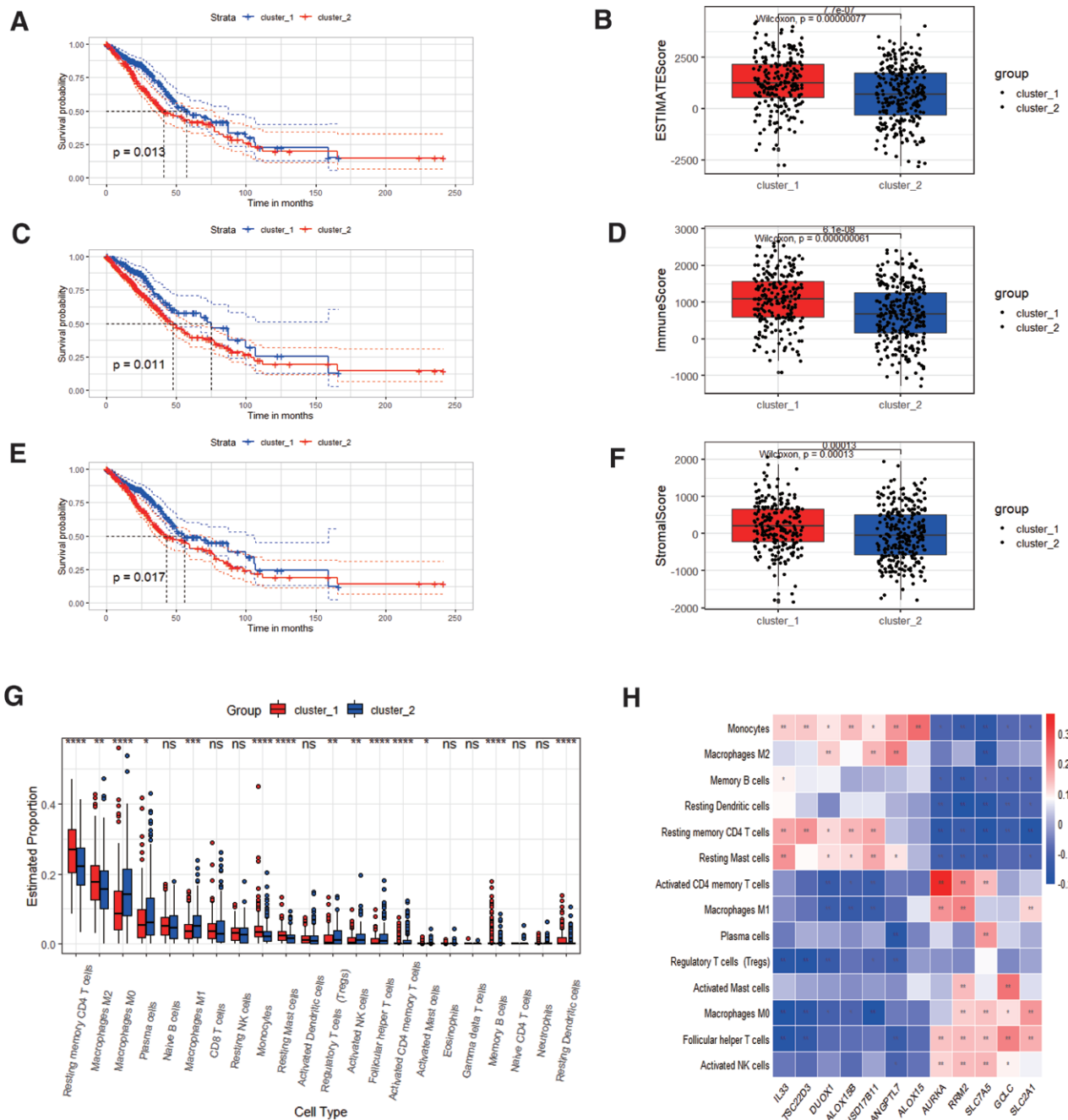


Figure 4. FRGs affect the TME in LUAD. (A) The relationship between EstimateScore and OS. (B) The level of EstimateScore in different subtypes. (C) The relationship between ImmuneScore and OS. (D) The level of ImmuneScore in different subtypes. (E) The relationship between StromalScore and OS. (F) The level of StromalScore in different subtypes. (G) Immune cell infiltration between different subtypes. (H) Correlation between differentially infiltrated immune cells and FRGs. FRGs = ferroptosis-related genes, LUAD = lung adenocarcinoma, OS = overall survival, TME = tumor microenvironment.

abundant cellular antioxidant in cells). Glutathione is the source of GPX4 synthesis, and its deficiency will cause inactivation of GPX4, promoting the accumulation of lipid peroxidation to a certain extent eventually inducing ferroptosis.^[28] Lipid metabolism is not only involved in the process of ferroptosis, but also an integral part for cancer cells.^[20] It provides cancer cells with energy for biological activities, biofilm components, lipid nutrients and oxidative stress environment, which contributes to rapid proliferation, prolonged survival and strong migratory invasive ability of cancer cells.^[21] These findings support the idea that cancer and ferroptosis interact. Inspired by this view, we used GO and KEGG enrichment analyses to identify genes that showed differential expression between LUAD

patients with poor OS rates and those with higher OS rates, and showed that some of these genes are bearers in the uptake and metabolic activities of fatty acids and arachidonic acid. In addition, DUOX1 and HSD17B11, which we identified, are also involved in these metabolic pathways. DUOX1 (dioxase 1) is a key protein in the NADPH oxidase family, whose main function is to produce reactive oxygen species.^[29] ROS have 2 sides, and can either promote or inhibit apoptosis.^[30] The expression of DUOX1 has been reported to be silent in lung cancer due to hypermethylation of its promoter.^[31] Silenced DUOX1 enhances lung cancer invasion and metastasis by promoting endothelial-mesenchymal transition.^[32] HSD17B11 is an important enzyme involved in lipid metabolism, especially steroid hormone

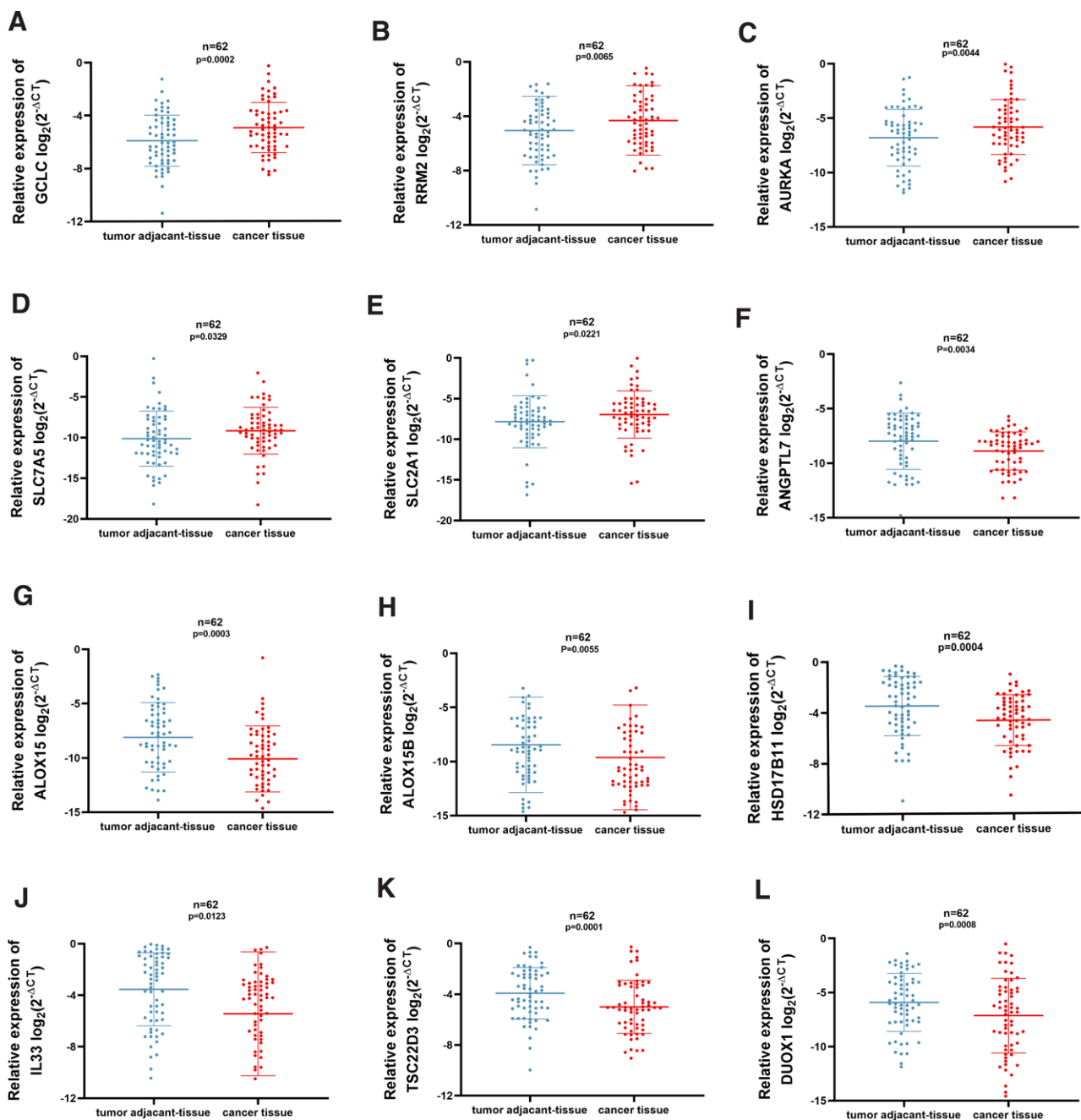


Figure 5. Verification of the expression levels of 12 FRGs in 62 LUAD patients. (A–E) Expression levels of GCLC, RRM2, AURKA, SLCTA5, and SLC2A1 in cancer tissues. (F–L) Expression levels of ANGPTL7, ALOX15, ALOX15B, HSD17B11, IL33, TSC22D3, and DUOX1 in cancer tissues ($*P < .05$). FRGs = ferroptosis-related genes, LUAD = lung adenocarcinoma.

metabolism. As a member of the family of short-chain dehydrogenases/reductases, it generally regulates lipid metabolism by targeting lipid droplets (LDs) related lipases, and one of the functions of LDs is to avoid fatty acid peroxidation.^[33] It has been reported that lipid metabolism is a novel molecular mechanism for tumor progression, and the expression of HSD17B11 can be enhanced by obesity-associated protein to promote LD formation in esophageal cancer, and YTHDF1 can reduce the translation rate of HSD17B11 and thus regulate the lipid metabolic process in tumors.^[34] Thus, we trust that HSD17B11 can affect the development of lung cancer by regulating the lipid metabolic process of ferroptosis as well, laying a theoretical foundation for new therapies for lung cancer.

TME is the environment on which tumor cells depend. It is enriched with a variety of immune cells, including T cells,

natural killer cells, and tumor-associated macrophages, which are beneficial for maintaining iron homeostasis.^[27] Wang et al found that CD8 + T cells could improve the efficacy of immunotherapy for tumors by regulating tumor ferroptosis, suggesting that ferroptosis could be a potential target for cancer immunotherapy.^[11] Immune cell recruitment mediated by DUOX1 not only phagocytosis of cancer cells to inhibit tumor growth and metastasis, but also the synergistic production of ROS by DUOX1 helps to kill cancer cells and enhance host defense.^[35,36] Restoration of DUOX1 expression in cancer cells with low DUOX1 levels significantly inhibited cancer cell growth and colony formation by inducing G2/M-phase cell cycle arrest and increasing reactive oxygen species production. Low DUOX1 expression tends to be associated with poorer prognosis, which is consistent with the findings of the present

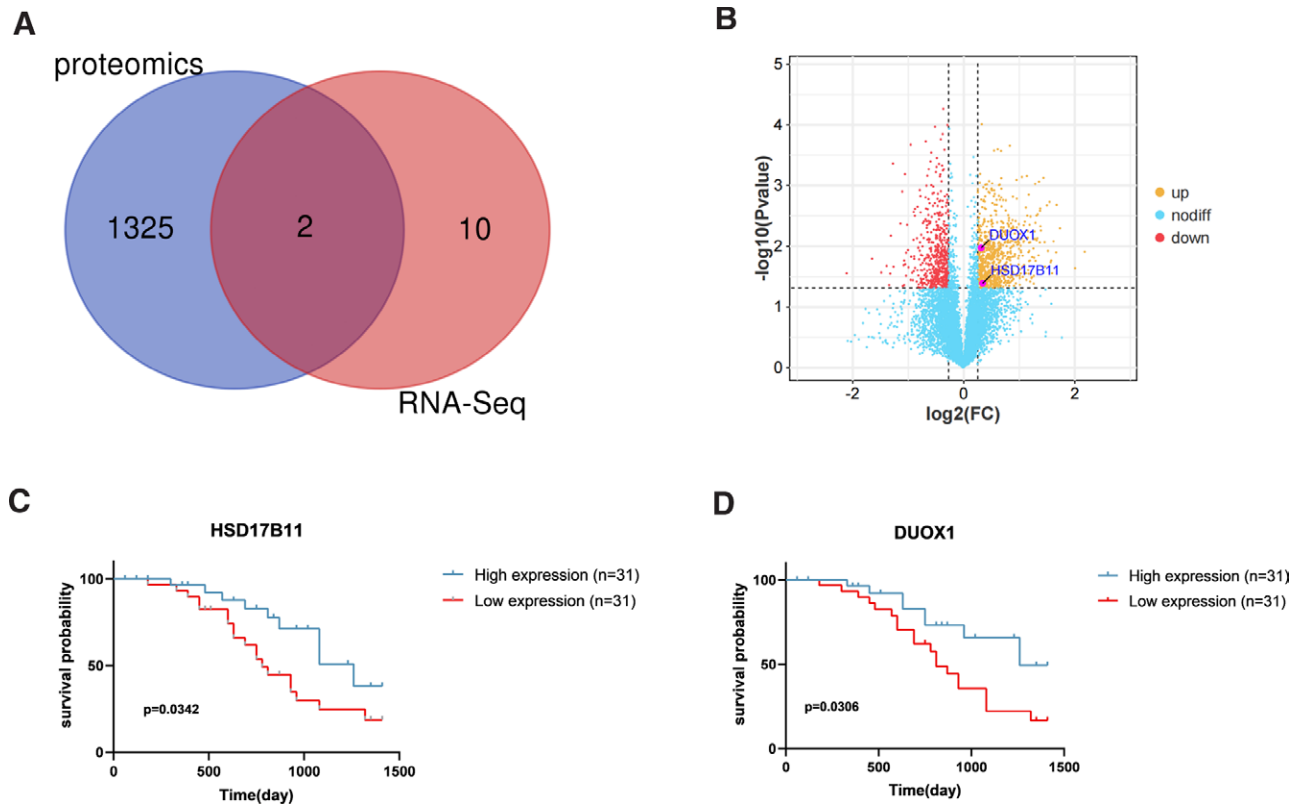


Figure 6. Validation of the prognosis of patients with tumors that have differential expression of FRGs. (A, B) Venn Diagram and volcano plot showing differences in RNA and protein levels between HSD17B11 and DUOX1. (C, D) The correlation between levels of HSD17B11 and DUOX1 and OS rates in LUAD patients, according to Kaplan–Meier curves ($P < .05$). FRGs = ferroptosis-related genes, LUAD = lung adenocarcinoma, OS = overall survival.

Table 2
Association of HSD17B11 and DUOX1 expression with clinical variables of LUAD.

Clinical variables	HSD17B11		P value	DUOX1		P value
	High	Low		High	Low	
All cases	31	31		31	31	
Gender			0.4404			0.7972
Male	20	16		17	19	
Female	11	15		14	12	
Age (yr)			>0.9999			0.7972
<60	18	18		17	19	
≥60	13	13		14	12	
Smoking status			0.7972			>0.9999
Smoker (No)	14	12		13	13	
Smoker (Yes)	17	19		18	18	
Diameter (cm)			0.2351			>0.9999
≤3	10	5		7	8	
>3	21	26		24	23	
T stage			0.0066*			0.1063
T1/T2	26	15		24	17	
T3/T4	5	16		7	14	
N stage			0.0262*			0.5824
N0	26	17		23	20	
N1–N3	5	14		8	11	
M stage			0.7802			0.0159*
M0	21	19		25	15	
M1	10	12		6	16	
Clinical stage			0.1196			0.0374*
I–IIa	16	9		17	8	
IIb–IV	15	22		14	23	

DUOX1 = dioxase 1, LUAD = lung adenocarcinoma.
 * $P < 0.05$ was considered statistically significant.

study, and increasing the expression level of DUOX1 in lung cancer and thus inhibiting cancer progression has the potential to be a new direction for immunotherapy. HSD17B11 was negatively correlated with tumor-infiltrating CD4+ and resting mast cells, and monocytes, and somatic copy number alterations may be largely responsible for it. This suggests that HSD17B11 is an independent potential prognostic biomarker for NSCLC and can be used to assess the level of immune cell infiltration in tumor tissues. Relatively low levels of HSD17B11 in LUAD tissues may signify a higher risk of tumor recurrence after treatment.

In conclusion, we confirmed the correlation between low expression of HSD17B11 and DUOX1 and poor OS in LUAD patients by combining bioinformatics analysis, proteomics, and multiplex analysis of clinical samples in this study. It was confirmed that the low expression of DUOX1 and HSD17B11 may suggest an increased tumor recurrence rate and decreased survival quality in LUAD patients. Targeting drugs that induce the expression of these 2 genes may be a new idea to consider. In addition, HSD17B11 lacks relevant research data in this area of ferroptosis, and our findings fill this gap. Notably, the molecular crosstalk through which pathways and downstream target genes HSD17B11 affect lung cancer is not yet clear to us and needs to be confirmed by further studies.

Acknowledgments

We thank Alison Inglis, PhD from Liwen Bianji (Edanz) (www.liwenbianji.cn) for editing the English text of a draft of this manuscript.

Author contributions

Conceptualization: Dong Wu.

Formal analysis: Youping Qiao.

Methodology: Yujuan Chen.

Resources: Zhu Liang, Dong Wu.

Software: Chunhui Wei, Jinye Xie.

Supervision: Jiayan Fang.

Visualization: Chunfeng Zhang.

Writing – original draft: Chunhui Wei, Lixia Li, Dong Wu.

Writing – review & editing: Chunhui Wei, Lixia Li, Dan Huang.

References

- [1] Siegel RL, Miller KD, Wagle NS, et al. Cancer statistics, 2023. *CA Cancer J Clin.* 2023;73:17–48.
- [2] Xu JY, Zhang C, Wang X, et al. Integrative proteomic characterization of human lung adenocarcinoma. *Cell.* 2020;182:245–61.e17.
- [3] Herbst RS, Morgensztern D, Boshoff C. The biology and management of non-small cell lung cancer. *Nature.* 2018;553:446–54.
- [4] Wang B, Jing T, Jin W, et al. KIAA1522 potentiates TNF α -NF κ B signaling to antagonize platinum-based chemotherapy in lung adenocarcinoma. *J Exp Clin Cancer Res.* 2020;39:170.
- [5] Jin J, Liu C, Yu S, et al. A novel ferroptosis-related gene signature for prognostic prediction of patients with lung adenocarcinoma. *Aging (Milano).* 2021;13:16144–64.
- [6] Liang C, Zhang X, Yang M, et al. Recent progress in ferroptosis inducers for cancer therapy. *Adv Mater.* 2019;31:e1904197.
- [7] Li L, Gao Q, Wang J, et al. Induction of ferroptosis by ophiopogonin-B through regulating the gene signature AURKA in NSCLC. *Front Oncol.* 2022;12:833814.
- [8] Zhao L, Zhou X, Xie F, et al. Ferroptosis in cancer and cancer immunotherapy. *Cancer Commun (Lond).* 2022;42:88–116.
- [9] Hangauer MJ, Viswanathan VS, Ryan MJ, et al. Drug-tolerant persister cancer cells are vulnerable to GPX4 inhibition. *Nature.* 2017;551:247–50.
- [10] Zhang C, Liu X, Jin S, et al. Ferroptosis in cancer therapy: a novel approach to reversing drug resistance. *Mol Cancer.* 2022;21:47.
- [11] Wang W, Green M, Choi JE, et al. CD8(+) T cells regulate tumour ferroptosis during cancer immunotherapy. *Nature.* 2019;569:270–4.
- [12] Wang Y, Zhang S, Bai Y, et al. Development and validation of ferroptosis-related LncRNA biomarker in bladder carcinoma. *Front Cell Dev Biol.* 2022;10:809747.
- [13] Zhao J, Huang X, Liu P, et al. Engineering alendronate-composed iron nanochelator for efficient peritoneal carcinomatosis treatment. *Adv Sci (Weinh).* 2022;9:e2203031.
- [14] Lu Z, Xiao B, Chen W, et al. The potential of ferroptosis combined with radiotherapy in cancer treatment. *Front Oncol.* 2023;13:1085581.
- [15] Zhu G, Huang H, Xu S, et al. Prognostic value of ferroptosis-related genes in patients with lung adenocarcinoma. *Thorac Cancer.* 2021;12:1890–9.
- [16] Zhou N, Bao J. FerrDb: a manually curated resource for regulators and markers of ferroptosis and ferroptosis-disease associations. *Database.* 2020;2020:1758–0463.
- [17] Yang L, Wu H, Jin X, et al. Study of cardiovascular disease prediction model based on random forest in eastern China. *Sci Rep.* 2020;10:5245.
- [18] Zheng PF, Liu F, Zheng ZF, et al. Identification MNS1, FRZB, OGN, LUM, SERP1NA3 and FCN3 as the potential immune-related key genes involved in ischaemic cardiomyopathy by random forest and nomogram. *Aging (Milano).* 2023;15:1475–95.
- [19] Oudkerk M, Liu S, Heuvelmans MA, et al. Lung cancer LDCT screening and mortality reduction - evidence, pitfalls and future perspectives. *Nat Rev Clin Oncol.* 2021;18:135–51.
- [20] Snaebjornsson MT, Janaki-Raman S, Schulze A. Greasing the wheels of the cancer machine: the role of lipid metabolism in cancer. *Cell Metab.* 2020;31:62–76.
- [21] Bian X, Liu R, Meng Y, et al. Lipid metabolism and cancer. *J Exp Med.* 2021;218:e20201606.
- [22] Wang Y, Wei Z, Pan K, et al. The function and mechanism of ferroptosis in cancer. *Apoptosis.* 2020;25:786–98.
- [23] Broderick L, Yokota SJ, Reineke J, et al. Human CD4+ effector memory T cells persisting in the microenvironment of lung cancer xenografts are activated by local delivery of IL-12 to proliferate, produce IFN- γ , and eradicate tumor cells. *J Immunol.* 2005;174:898–906.
- [24] Kaesler S, Wölbing F, Kempf WE, et al. Targeting tumor-resident mast cells for effective anti-melanoma immune responses. *JCI Insight.* 2019;4:e125057.
- [25] Gu Z, Liu T, Liu C, et al. Ferroptosis-strengthened metabolic and inflammatory regulation of tumor-associated macrophages provokes potent tumoricidal activities. *Nano Lett.* 2021;21:6471–9.
- [26] Xu H, Ye D, Ren M, et al. Ferroptosis in the tumor microenvironment: perspectives for immunotherapy. *Trends Mol Med.* 2021;27:856–67.
- [27] Recalcati S, Locati M, Marini A, et al. Differential regulation of iron homeostasis during human macrophage polarized activation. *Eur J Immunol.* 2010;40:824–35.
- [28] Harris IS, Endress JE, Coloff JL, et al. Deubiquitinases maintain protein homeostasis and survival of cancer cells upon glutathione depletion. *Cell Metab.* 2019;29:1166–81.e6.
- [29] Leto TL, Geiszt M. Role of Nox family NADPH oxidases in host defense. *Antioxid Redox Signal.* 2006;8:1549–61.
- [30] Ashtawi NM, Sarr D, Rada B. DUOX1 in mammalian disease pathophysiology. *J Mol Med (Berl).* 2021;99:743–54.
- [31] Luxen S, Belinsky SA, Knaus UG. Silencing of DUOX NADPH oxidases by promoter hypermethylation in lung cancer. *Cancer Res.* 2008;68:1037–45.
- [32] Little AC, Sham D, Hristova M, et al. DUOX1 silencing in lung cancer promotes EMT, cancer stem cell characteristics and invasive properties. *Oncogenesis.* 2016;5:e261.
- [33] Liu Y, Xu S, Zhang C, et al. Hydroxysteroid dehydrogenase family proteins on lipid droplets through bacteria, *C. elegans*, and mammals. *Biochim Biophys Acta Mol Cell Biol Lipids.* 2018;1863:881–94.
- [34] Duan X, Yang L, Wang L, et al. m6A demethylase FTO promotes tumor progression via regulation of lipid metabolism in esophageal cancer. *Cell Biosci.* 2022;12:60.
- [35] Little AC, Sulovari A, Danyal K, et al. Paradoxical roles of dual oxidases in cancer biology. *Free Radic Biol Med.* 2017;110:117–32.
- [36] Candel S, de Oliveira S, López-Muñoz A, et al. Tnfa signaling through tnfr2 protects skin against oxidative stress-induced inflammation. *PLoS Biol.* 2014;12:e1001855.